Lack of Lymphatics and Lymph Node–Mediated Immunity in Choroidal Neovascularization

Shintaro Nakao,[1–3] Souska Zandi,[1,2,4] Ri-ichiro Kohno,[3] Dawei Sun,[1,2] Takahito Nakama,[3] Keijiro Ishikawa,[3] Shigeo Yoshida,[3] Hiroshi Enaida,[3] Tatsuro Ishibashi,[3] and Ali Hafezi-Moghadam[1,2]

[1]Center for Excellence in Functional and Molecular Imaging, Brigham and Women's Hospital, and Department of Radiology, Harvard Medical School, Boston, Massachusetts
[2]Angiogenesis Laboratory, Massachusetts Eye and Ear Infirmary, and Department of Ophthalmology, Harvard Medical School, Boston, Massachusetts
[3]Department of Ophthalmology, Graduate School of Medical Sciences, Kyushu University, Fukuoka, Japan
[4]Department of Ophthalmology, Geneva University Hospitals, Geneva, Switzerland

Correspondence: Ali Hafezi-Moghadam, Brigham and Women's Hospital, 221 Longwood Avenue, 3rd Floor, Boston, MA 02115; ahm@bwh.harvard.edu.

Submitted: June 5, 2012
Accepted: April 2, 2013

Citation: Nakao S, Zandi S, Kohno R-I, et al. Lack of lymphatics and lymph node–mediated immunity in choroidal neovascularization. *Invest Ophthalmol Vis Sci*. 2013;54;3830–3836. DOI:10.1167/iovs.12-10341

Purpose. Inflammation and immune cells regulate choroidal neovascularization (CNV) and could become therapeutic targets in age-related macular degeneration (AMD). Lymphangiogenesis is a key component of various inflammatory diseases. Whether lymphangiogenesis and lymph node–mediated immunity are involved in the pathogenesis of AMD is not understood.

Methods. To investigate lymphangiogenesis in CNV, we generated CNV in animals by laser and studied surgically removed CNV membranes from uveitis and AMD patients. Immunohistochemistry was performed with lymphatic vessel endothelial hyaluronate receptor 1 (LYVE-1) and podoplanin antibodies. VEGF-C and VEGFR-3 expressions were examined with immunohistochemistry and Western blotting. To examine the role of lymph node in CNV, we lasered lymphotoxin alpha–deficient mice (*LTα*−/−) and measured the CNV volume.

Results. Immunohistochemistry showed that LYVE-1(+) macrophages infiltrated in acutely induced CNV, although lymphatic tubes did not form. CNV membranes from patients did not show LYVE-1(+)podoplanin(+) vessels, suggesting the lack of lymphangiogenesis in AMD and uveitis. Western blots and immunostaining revealed VEGF-C and VEGFR-3 expression in CNV lesions, mainly in macrophages and angiogenic endothelial cells. Using fluorescent microsphere tracers, we show a path for cellular migration from the eye to the cervical lymph nodes (LNs) during CNV. However, CNV injury did not cause LN swelling. CNV volume did not differ between wild-type and LN-deficient mice, suggesting that LN is not a key component of early CNV formation.

Conclusions. Laser-induced CNV is not primarily dependent on acquired immunity, nor does the fundus injury affect peripheral LNs. Our results reveal a previously unknown cellular connection between the ocular fundus and the cervical LNs. This connection that in function resembles lymphatics is actively utilized in CNV.

Keywords: macrophage, LYVE-1, VEGFR-3, VEGF-C, AMD, uveitis

The role of immune cells in choroidal neovascularization (CNV) is well established.[1–3] Infiltrating macrophages and dendritic cells release growth factors (GFs), such as the vascular endothelial growth factor (VEGF), that promote angiogenesis.[4,5] Following inflammatory angiogenesis, lymphangiogenesis occurs.[6] Recently, we showed that angiogenic vessels and infiltrated leukocytes regulate lymphangiogenesis.[6,7] During inflammation and immune reaction, macrophages and dendritic cells enter lymphatics to return to lymph nodes (LNs).[8,9] However, the contribution of lymphatics and LNs to CNV formation is unknown.

Nearly all tissues in the body are vascularized with blood and lymphatic vessels.[10] Among the exceptions are cornea, epidermis, and cartilage that do not have blood or lymphatic vessels, whereas brain and retina are highly vascularized with blood vessels, yet are alymphatic.[10] Whether the choroid in the eye contains lymphatics has been controversial.[11] Histologic studies in the 1990s suggested the existence of lymphatics and lymphatic-like structures.[12–14] A study about avian eye indicated that the lacunae of the choroid represented a system with short lymphatic vessels, which reach the choriocapillaris.[12] Other studies using electron microscopy showed in the choroid of monkeys vessels with lymphatic features, such as anchoring filaments and discontinuous external basement lamina.[13,14] More recent immunohistochemical studies, performed after the discovery of specific lymphatic vessel markers, showed lymphatic vessel endothelial hyaluronate receptor 1 (LYVE-1)(+) macrophages but no LYVE-1(+) lymphatic vessel in human or mouse choroid.[15,16] However, whether under pathologic conditions choroid and retina express lymphatic vessels is unknown.

VEGF-A inhibition is a potent therapy for CNV in age-related macular degeneration (AMD) patients. VEGF-A signaling through the VEGFR-2 mainly drives angiogenesis. In contrast,

VEGF-C signaling through the VEGFR-3 drives lymphangiogenesis,[10,17] and under some conditions also angiogenesis.[18] The contribution of VEGF-C through VEGFR-3 signaling in AMD pathogenesis has not been studied.

Materials and Methods

Animals

All animal experiments were approved by the Animal Care Committee of the Massachusetts Eye and Ear Infirmary. Homozygous lymphotoxin alpha–deficient mice (*LTα−/−*; stock number, 002258; The Jackson Laboratory, Bar Harbor, ME) on a C57BL/6 background and C57BL/6 mice (The Jackson Laboratory) were housed and cared for according to institutional guidelines. Six- to 12-week-old mice were used for experiments.

Human Tissue

CNV tissues were excised from two uveitis and four AMD patients. The study followed the guidelines of the Declaration of Helsinki. Institutional review boards granted approval for allocation and histologic analysis of specimens.

Laser-Induced Choroidal Neovascularization

To induce CNV, C57BL/6 mice were anesthetized and pupils were dilated with 2.5% phenylephrine and 0.8% tropicamide. Using a 532-nm laser (Oculight GLx, IRIDEX, Mountain View, CA), a slit-lamp delivery system, and a cover glass as a contact lens, four spots (100 mW, 50 μm, 100 ms) were placed in each eye. The lesions were located at 3, 6, 9, and 12 o'clock meridians centered on the optic nerve head and located 2 to 3 disc diameters from the optic nerve head. Development of a bubble under laser confirmed the rupture of the Bruch's membrane. Eyes showing hemorrhage were excluded from experiments. Seven or 14 days after laser injury, the size of the CNV lesions was measured in choroidal flat mounts. Briefly, mice were anesthetized and perfused through the left ventricle with PBS, followed by 5 mL of 5% fluorescein isothiocyanate-dextran (FD2000S; Sigma-Aldrich, St. Louis, MO) in 1% gelatin. The anterior segment and retina were removed from the eyecup. The remaining retinal pigment epithelium (RPE)–choroid–sclera complex was flat mounted, after relaxing radial incisions, using mounting medium (FM 100119; Thermo Fisher Scientific, Inc., Waltham, MA) and coverslips. Micrographs of the choroidal complex were taken with a laser scanning confocal microscope (Leica TCS SP2 microscope; Leica Microsystems GmbH, Wetzlar, Germany). The area of the lesions was quantified. The magnitude of the CNV lesions was determined by measuring the hyperfluorescent area with a commercial software package (Openlab software; Improvision Software/PerkinElmer, Inc., Waltham, MA).

Whole-Mount Immunofluorescence

The animals' eyes were enucleated and fixed with 4% paraformaldehyde for 30 minutes at 4°C. For whole-mount preparation the retinas or choroids were microsurgically exposed by removing other portions of the eye. Tissues were washed with PBS three times for 5 minutes and then placed in methanol for 20 minutes. Tissues were incubated overnight at 4°C with antimouse CD31 mAb (5 μg/mL, 550274; BD Pharmingen, Inc., San Diego, CA), antimouse LYVE-1 Ab (4 μg/mL, 103-PA50AG; RELIATech GmbH, Braunschweig, Germany) and antimouse F4/80 Cy5-conjugated Ab (10 μg/mL, MCA497A647T; AbD Serotec, Oxford, UK) diluted in PBS containing 10% goat serum and 1% Triton X-100. Tissues were washed four times for 20 minutes in PBS followed by incubation with Alexa Fluor488 goat antirat IgG (20 μg/mL, A11006; Invitrogen, Carlsbad, CA) and Alexa Fluor546 goat antirabbit IgG (20 μg/mL, A11035; Invitrogen) overnight at 4°C. Corneal flat mounts were prepared on glass slides using a mounting medium (TA-030-FM Mountant Permafluor; Lab Vision Corporation/Thermo Fisher Scientific, Inc., Kalamazoo, MI). The flat mounts were examined by fluorescence microscopy (Leica TCS SP2 laser scanning confocal microscope; Leica Microsystems GmbH) and digital images were recorded with standardized illumination and contrast. The number of LYVE-1(+) cells was counted in whole retinas under fluorescence microscopy.

Immunohistochemistry of Mouse CNV

The eyes were harvested and snap-frozen in optimal cutting temperature (OCT) compound (Sakura Finetechnical, Tokyo, Japan). Sections (10 μm) were prepared, air-dried, and fixed in ice-cold acetone for 10 minutes. The sections were blocked with 3% nonfat dried Milk bovine working solution (M7409; Sigma-Aldrich) and stained with antimouse CD31 (1/50, 550282; BD Pharmingen), antimouse LYVE-1 (1 μg/mL, 103-PA50AG; RELIATech GmbH), anti-VEGF-C (1/200, sc7132; Santa Cruz Biotechnology, Santa Cruz, CA), antimouse CD11b (1/200, 550282; BD Pharmingen) or anti-VEGFR-3 (1/200, sc321; Santa Cruz Biotechnology). After an overnight incubation, sections were washed and stained for 20 minutes with Alexa Fluor488 goat antirat IgG (10 μg/mL, A11006; Invitrogen), Alexa Fluor546 goat antirabbit IgG (10 μg/mL, A11035; Invitrogen) and Alexa Fluor647 rabbit antigoat IgG (10 μg/mL, A21446; Invitrogen).

Immunohistochemistry of Human CNV

Surgically removed CNV membranes were fixed in 4% paraformaldehyde, embedded in paraffin wax, cut into 5-μm sections, and deparaffinized according to standard procedures. The sections were blocked with peroxidase in 1% H_2O_2/methanol for 5 minutes. Heat-induced epitope retrieval was performed by immersing sections of tissue in citrate buffer (pH 6.0). Tissues were incubated overnight at 4°C with antihuman LYVE-1 Ab (1/200, 102-PA50AG; RELIATech GmbH), antihuman podoplanin (D2-40) Ab (1/100, M3629; Dako Denmark A/S, Glostrup, Denmark) or antihuman cytokeratin 19 (1/50, sc-33119; Santa Cruz Biotechnology) in PBS in a humidified chamber and incubated with peroxidase-labeled secondary antibody (Envision System; Dako Denmark A/S) or Alexa Fluor488 goat antimouse IgG (10 μg/mL, A11001; Invitrogen), and Alexa Fluor647 goat antirabbit IgG (10 μg/mL, A21244; Invitrogen) or Alexa Fluor647 rabbit antigoat IgG (10 μg/mL, A21446; Invitrogen) following the primary antibodies. Horseradish peroxidase activity was visualized with 3,3′-diaminobenzidine tetrahydrochloride (DAB; Merck, Darmstadt, Germany) to give the reaction product a red color, and then the sections were counterstained with hematoxylin. Either nonimmune rabbit IgG or nonimmune mouse IgG of each isotype was also used instead of the respective primary antibodies as a negative control.

Western Blot Analysis

To obtain tissues, animals were perfused with PBS and eyes were enucleated immediately after perfusion. Choroids–RPE complexes were microsurgically isolated and placed in 100 μL of lysis buffer (mammalian cell lysis kit MCL1; Sigma-Aldrich) supplemented with protease and phosphatase inhibitors

Investigative Ophthalmology & Visual Science

(P2850, P5726, P8340; Sigma-Aldrich), and sonicated. The lysate was centrifuged (12,000 rpm, 15 minutes, 4°C) and the supernatant was collected. Lysates were subjected to sodium dodecyl sulfate–polyacrylamide gel electrophoresis and transferred to commercial membranes (Immobilon; Millipore, Bedford, MA). Blots were incubated with anti-VEGFR-2 (1/1000, #2479; Cell Signaling, Beverly, MA), anti-VEGFR-3 (1/200, sc321; Santa Cruz Biotechnology), VEGF-D (1/200, sc13685; Santa Cruz Biotechnology) or anti-β-tubulin (1:1000, ab11308; Abcam, Cambridge, MA) and visualized with a secondary antibody coupled to horseradish peroxidase (Amersham, Buckinghamshire, UK) and enhanced chemiluminescence system.

Tracing of Fluorescent Imaging Probes

Fluorescent microspheres (1×10^4, 2 μm; Polysciences, Inc., Warrington, PA) were injected into the vitreous cavity of lasered or normal control mice 1 day after laser injury. Four days after laser induction, we harvested cervical, axial/branchial, and inguinal lymph nodes and the harvested lymph nodes were examined by fluorescence microscopy.

Statistical Analysis

All values are expressed as mean ± SEM. Data were analyzed by Student's *t*-test. Differences between the experimental groups were considered statistically significant (*) when the probability value, *P*, was <0.05.

Results

Examination of Lymphatics in Laser-Induced Choroidal Neovascularization and CNV Membranes From Patients

To investigate whether lymphangiogenesis occurs in the retina or choroids during CNV, we performed laser-induced CNV in C57BL/6 mice and immunostained cryosections and whole-mounts for LYVE-1 and CD31. As a positive control, corneas of normal animals were stained and examined under the same conditions. Corneal limbus of C57BL/6 mice contained LYVE-1(+) lymphatic vessels (Fig. 1A), in line with our previous report.[17] In the cryosections of normal and lasered mice, LYVE-1(+) tubes were not observed in the retinas and choroids (Fig. 1A). Whole-mount staining showed LYVE-1(+) cells in the CD31(+) CNV lesions, but these LYVE-1(+) cells were not in a tube formation that would indicate the shape of a lymphatic vessel (Fig. 1B). Some of the LYVE-1(+) cells in the CNV lesions were also positive for the macrophage marker, F4/80. The LYVE-1(+)F4/80(+) cells were observed in the retinas of lasered as well as normal animals (Figs. 1C, 1D). In lasered eyes significantly more LYVE-1(+) macrophages were found than in normal eyes (Fig. 1E). These data strongly suggest that lymphangiogenesis does not occur during CNV. However, LYVE-1(+) macrophages infiltrate into the retina during CNV.

Next we examined whether CNV membranes from uveitis and AMD patients contain lymphatic vessels. To visualize the lymphatic vessels in the CNV membrane, we stained for podoplanin and LYVE-1. We observed podoplanin(+) cells and podoplanin(+) tube structures, although these cells did not show LYVE-1 expression (Fig. 1F). Interestingly, podoplanin expression was found in the RPE cells (Fig. 1G), as previously shown in normal murine eyes.[19] Furthermore, podoplanin was expressed in cytokeratin(+) cells, that could be RPE cells in CNV (Fig. 1H). These data suggest that CNV membranes do not contain typical lymphatic vessels.

Expression of Lymphangiogenesis-Related Factors in Laser-Induced CNV

To investigate the expression of the lymphangiogenesis-related members of the VEGF family, VEGFR-2, VEGFR-3, and VEGF-C, in CNV, we measured these proteins in Western blot. VEGF-C but not VEGFR-2 or VEGFR-3 were increased in the choroids at day 3 and day 7 during CNV formation (Fig. 2A). Interestingly, the active forms of VEGF-C and -D (21 and 31 kDa) were expressed at higher levels in the CNV eyes than in normal controls (Fig. 2A). To identify the source and locations of the VEGF-C and VEGFR-3 in CNV, we performed immunohistochemistry for VEGF-C and VEGFR-3 in combination with CD31, CD11b, and LYVE-1. VEGF-C and VEGFR-3 are expressed in CD11b(+) cells, as well as in CD31(+) CNV, suggesting that VEGF-C is expressed in macrophages as well as in CNV (Figs. 2B–E).

Contribution of Lymph Nodes to Laser-Induced CNV

To examine whether laser-induced CNV causes an inflammatory reaction in the peripheral LNs, we harvested the cervical, axial, and inguinal lymph nodes and measured their size during CNV formation. There was no appreciable difference in size or gross morphology between the cervical, axial, and inguinal lymph nodes from animals with CNV compared with normal (Figs. 3A, 3B).

To further examine whether the peripheral LNs are involved in CNV formation, we next explored a potential cellular migration route from the vitreous cavity to the peripheral LNs using fluorescent microspheres (MSs) in lasered and normal control animals. At day 4 after laser induction we harvested peripheral LNs from three different locations to examine potential accumulation of the injected MS to the LNs. The injected MSs were found in cervical LNs of lasered mice but not in normal controls, indicating a to-date unknown cellular path from the fundus to the cervical LNs, although apparently not to the other nodes (Figs. 3C, 3D). Remarkably, this cellular path was utilized, as indicated by the MS accumulation in the cervical LNs, during the CNV, although not under normal conditions.

Next to examine whether peripheral LNs influence CNV formation we performed laser injury in *LTα–/–* mice that are lymph node deficient. CNV volume in *LTα–/–* mice did not differ significantly from that in wild-type mice, 7 or 14 days after laser injury (Figs. 3E–H). These data indicate that laser-induced CNV in mice is independent of LNs, despite the existence of the newly described route that connects the vitreous cavity with the cervical LNs.

Discussion

VEGF-C activation of VEGFR-3 induces lymphangiogenesis in various tissues, including the cornea.[17,20] The role of these factors in CNV is not understood. We studied the expression of VEGF-C and VEGFR-3 in normal and CNV eyes and found VEGF-C to be upregulated in experimental CNV. However, despite higher levels of VEGF-C in CNV, we did not find signs of lymphangiogenesis, such as LYVE-1– or podoplanin- positive tubes, in the lasered mice or human tissues. Our data are in line with a similar observation in uveal melanoma.[21] Since VEGFR-3 is expressed on macrophages and angiogenic vessels, VEGFR-3 signaling likely also contributes to CNV.[18,22] However, the detailed role of the VEGF-C/VEGFR-3 pathway in AMD has not been elucidated.

The first AMD treatment, macugen (pegaptanib), selectively blocks the 164 isoform of VEGF-A.[23] The subsequently

Investigative Ophthalmology & Visual Science

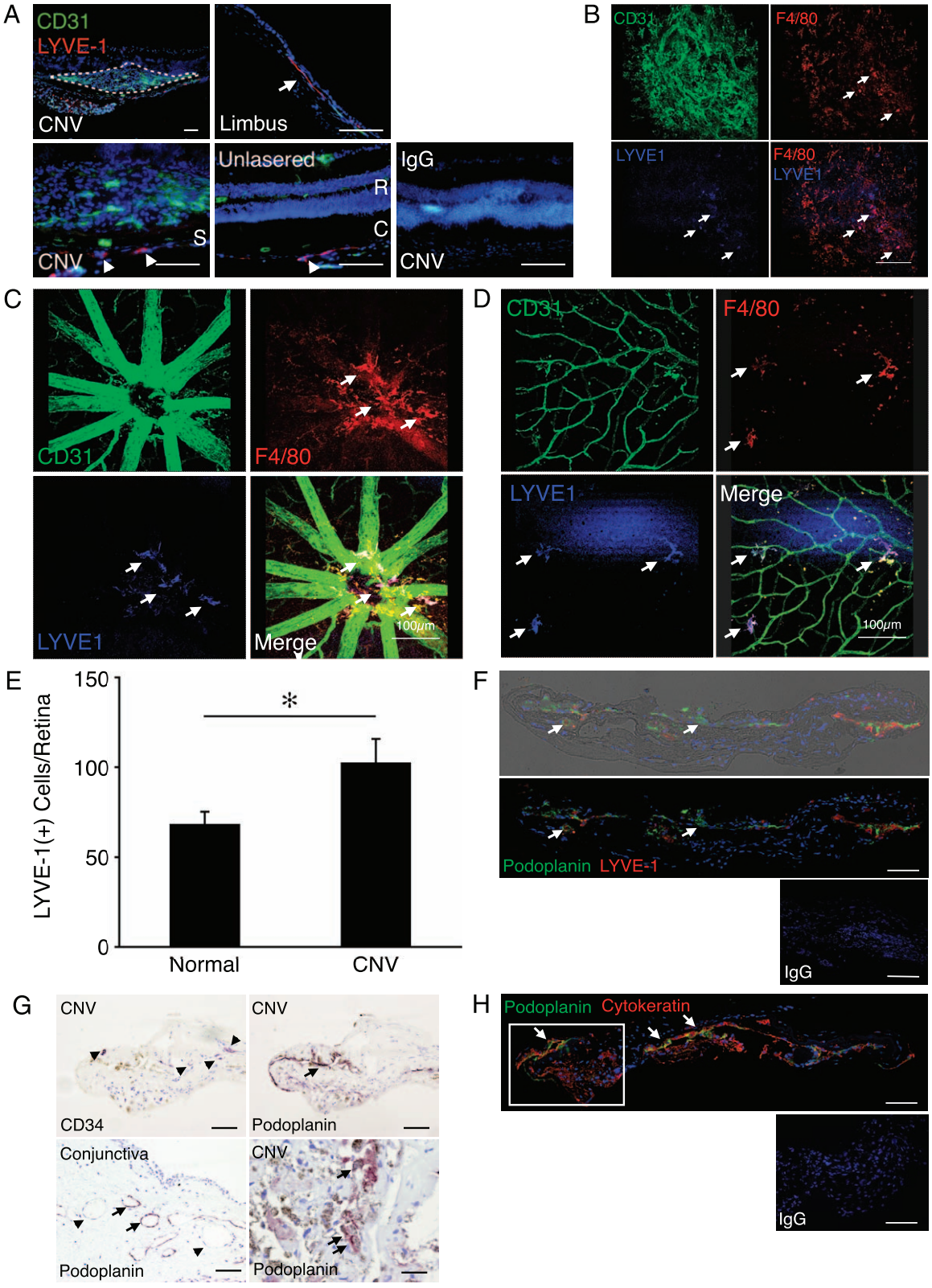

Figure 1. Lymphatic markers in the mouse CNV model and in human CNV membranes. (**A**) Double immunostaining of laser-induced CNV (day 7) (*left*), corneal limbus (*top right*), and normal retina (R) and choroid (C) with antibodies against CD31 (*green*), LYVE-1 (*red*), and DAPI (*blue*). *Dotted circle* indicates CNV lesion (*top left*). *Arrow* indicates flat lymphatic vessel (*top right*). *Arrowheads* indicates reported LYVE-1(+) single cells in sclera (S).[16] The specificity of staining is confirmed by the absence of staining with an isotype control IgG. *Bar*: 50 μm. (**B–D**) Triple staining of CNV (**B**), retina around disc (**C**), and retina around the equator (**D**) in lasered mice for endotheliums (CD31), macrophages (F4/80), and LYVE-1. *Arrows* indicate LYVE-1(+)F4/80 (+) macrophages. *Bar*: 100 μm. (**E**) Quantitation of the number of LYVE-1(+)F4/80 (+) macrophages in the whole retina of lasered and normal control mice at day 7 ($n = 6$ and $n = 8$). (**F**) Immunostaining of surgically removed CNV membrane (AMD) with podoplanin (*green*) and LYVE-1 (*red*) antibodies. *Arrows* indicate podoplanin(+)LYVE-1(−) tube-like structures. The specificity of staining is confirmed by the

Investigative Ophthalmology & Visual Science

absence of staining with an isotype control IgG. *Bar*: 100 μm. (**G**) Immunostaining of surgically removed CNV membrane (uveitis) or human conjunctiva with CD34 or podoplanin Ab. *Red staining* (*arrows*) indicates podoplanin expression in RPE cells. *Arrowheads* indicate podoplanin (–) blood vessels in conjunctiva. *Bar*: 50 μm. (**H**) Immunostaining of surgically removed CNV membrane (uveitis) with podoplanin (*green*) and keratin (*red*) Ab. *Arrows* indicate podoplanin expression in parts of RPE cells. *Rectangle* shows the same part in Figure 2G (*top*). *Bar*: 100 μm.

introduced AMD treatment, lucentis (ranibizumab), blocks all VEGF-A isoforms.[24] Inhibition of all VEGF-A isoforms by lucentis showed a better clinical result than the specific inhibition of the 164 isoform, suggesting that broader inhibitors might be more beneficial.[25] Recently, a new VEGF inhibitor, Eylea (aflibercept; VEGF trap-eye), was added to the assortment of the AMD therapeutics.[26] Eylea broadly traps PlGF, VEGF-A, and VEGF-B, but not VEGF-C and VEGF-D. Considering the potential role of VEGF-C to CNV, it is reasonable to expect a better clinical performance of Eylea compared with lucentis. Future clinical studies will have to address the efficacy of these inhibitors.

VEGF-C causes lymphangiogenesis.[27] For instance, in the corneal micro pocket assay, implantation of a VEGF-C pellet causes lymphangiogenesis; however, the new sprouts originate from the preexisting limbal lymphatics.[17] In the posterior section of the eye there are no known conventional lymphatic structures from which new sprouts would originate.[15,16] This could be the reason that, despite the existence of VEGF-C, no new lymphatic vessels grow during CNV.

Similar to other tissues, also in the retina regulation of fluid balance and immunity is needed. Lymphatics are critical for fulfillment of these important functions. The existence of conventional lymphatics in the choroid remains controversial.[12–16] Our data indicate that conventional lymphatic vessels do not exist in the choroids, even though choriocapillary might fulfill lymphatic-like functions.[14,15] It is also feasible that choroids constitute a unique lymphatic system that unlike conventional lymphatics does not express LYVE-1 and podoplanin. Recently, we introduced that lymphatic vessels contain

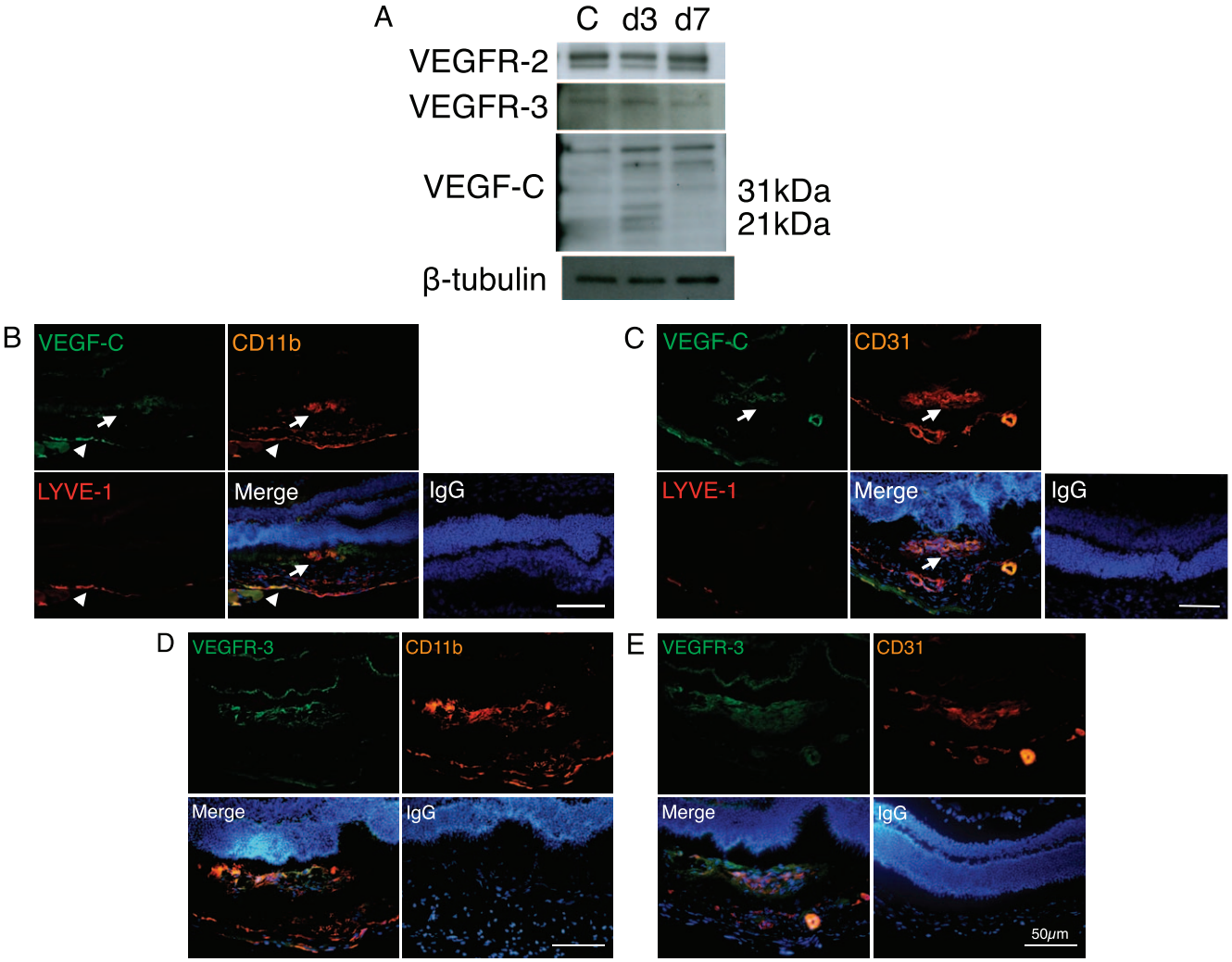

Figure 2. VEGF-C and VEGFR-3 expression in mouse CNV model. (**A**) Representative Western blot samples from lasered and normal control choroids–RPE complex (days 3 and 7) of mice with α-VEGFR-2, VEGFR-3, and VEGF-C antibodies, showing upregulation of matured VEGF-C in lasered CNV (day 3). (**B**, **C**) Triple immunostaining of CNV at day 3 (**B**) and day 7 (**C**) with antibodies against VEGF-C (*green*), CD11b (**B**), or CD31 (**C**) (*orange*), LYVE-1 (*red*), and DAPI (*blue*). *Arrow* (**B**) indicates VEGF-C expression in CD11b(+)LYVE-1(–) cells in CNV lesion. *Arrowhead* (**B**) indicates VEGF-C expression in CD11b(+)LYVE-1(+) cells in sclera. *Arrow* (**C**) indicates VEGF-C expression in CD31(+)LYVE-1(–) CNV in CNV. *Bar*: 50 μm. (**D**, **E**) Triple immunostaining of CNV at day 7 with antibodies against VEGFR-3 (*green*), CD11b (**D**), or CD31 (**E**) (*orange*), and DAPI (*blue*).

Investigative Ophthalmology & Visual Science

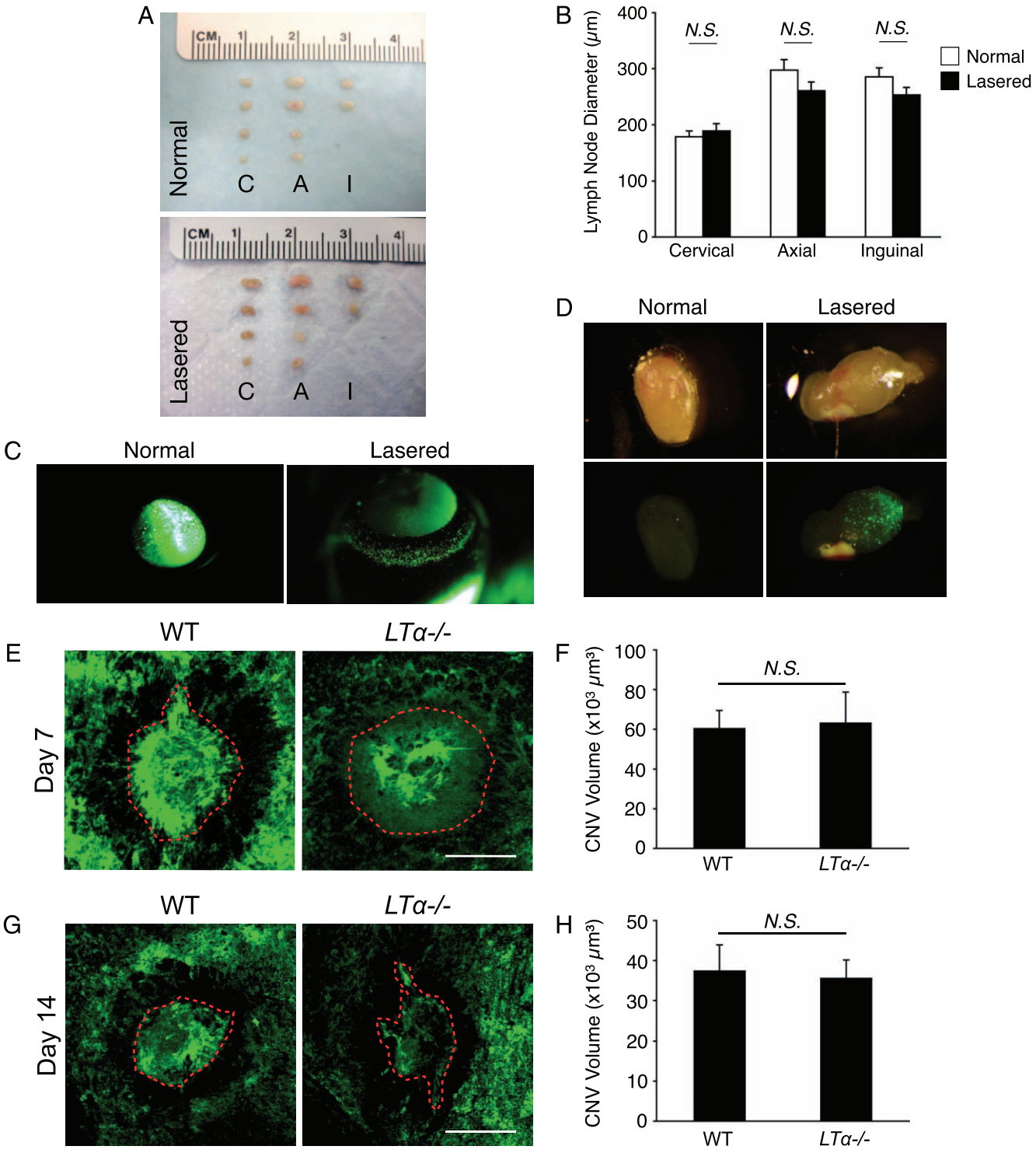

Figure 3. Lymph node and CNV. **(A)** Representative pictures of cervical (C), axial (A), and inguinal (I) lymph nodes from lasered and normal control mice (day 7). **(B)** Quantitative analysis of lymph node maximal diameter ($n = 6$). **(C, D)** Representative pictures of eye **(C)** and cervical **(D)** lymph nodes from lasered and normal control mice ($n = 4$). **(E–H)** Representative micrographs of CNV lesions at day 7 **(E)** and day 14 **(G)** in choroidal flat mounts from wild-type mice or *LTα–/–* mice. *Red dashed line*, extent of the CNV lesions filled with FITC-dextran in flat-mounted choroids. *Scale bar*: 100 μm. Quantitative analysis of CNV volume in each group at day 7 **(F)** and day 14 **(H)**. *Scale bar*: 100 μm.

LYVE-1 negative endothelium that serves as reentry ports for immune cells.[9]

AMD has many aspects of inflammatory and immune diseases.[28] Recruitment of immune cells is an essential part of CNV formation.[28] Little is known, however, how immune cells exit the eye. To leave the tissue, macrophages and dendritic cells enter into lymphatic vessels and access regional LNs and regulate the immune system.[8] Since there are no known paths for exit of immune cells out of the posterior section of the eye, the role of immunity in AMD has not been studied. This study reveals a previously unknown path for immune cells to reach the regional LNs in spite of the absence

Investigative Ophthalmology & Visual Science

of classic lymphatics. Although immune cells might enter the lymphatic vessels of the optic nerve meninges, the exact mechanism has not been understood.[29]

Our studies further indicate that LN deficiency does not affect angiogenesis in the experimental posterior eye injury in the first 2 weeks. Inflammation generally increases lymph node size.[30] Therefore, we had hypothesized that CNV-related inflammation might cause lymph node differences. However, we found that experimental CNV does not affect the regional LNs. The role of immunity in later stages of CNV still needs to be investigated, because it is feasible that immunity might play a role in later stages, such as fibrosis or regression. However, it is safe to conclude that the acute inflammatory response in laser-induced CNV is not primarily through acquired immunity. This might be a distinction of this acute model of CNV from the human AMD.

Acknowledgments

The authors thank members of the Malaysian Palm Oil Board and the BrightFocus Foundation.

Supported by NIH Grant AI050775 (AH-M), an overseas Research Fellowship Award from Bausch & Lomb, a Fellowship Award from the Japan Eye Bank Association and Tear Film and Ocular Surface Society, and a Young Investigator Fellowship (to SN under the mentorship of AH-M).

Disclosure: **S. Nakao**, None; **S. Zandi**, None; **R.-I. Kohno**, None; **D. Sun**, None; **T. Nakama**, None; **K. Ishikawa**, None; **S. Yoshida**, None; **H. Enaida**, None; **T. Ishibashi**, None; **A. Hafezi-Moghadam**, None

References

1. Nakai K, Fainaru O, Bazinet L, et al. Dendritic cells augment choroidal neovascularization. *Invest Ophthalmol Vis Sci*. 2008;49:3666–3670.
2. Tsutsumi C, Sonoda KH, Egashira K, et al. The critical role of ocular-infiltrating macrophages in the development of choroidal neovascularization. *J Leukoc Biol*. 2003;74:25–32.
3. Apte RS, Richter J, Herndon J, Ferguson TA. Macrophages inhibit neovascularization in a murine model of age-related macular degeneration. *PLoS Med*. 2006;3:e310.
4. Nakao S, Kuwano T, Tsutsumi-Miyahara C, et al. Infiltration of COX-2-expressing macrophages is a prerequisite for IL-1 beta-induced neovascularization and tumor growth. *J Clin Invest*. 2005;115:2979–2991.
5. Nakao S, Noda K, Zandi S, et al. VAP-1-mediated M2 macrophage infiltration underlies IL-1beta- but not VEGF-A-induced lymph- and angiogenesis. *Am J Pathol*. 2011;178:1913–1921.
6. Nakao S, Zandi S, Hata Y, et al. Blood vessel endothelial VEGFR-2 delays lymphangiogenesis: an endogenous trapping mechanism links lymph- and angiogenesis. *Blood*. 2011;117:1081–1090.
7. Watari K, Nakao S, Fotovati A, et al. Role of macrophages in inflammatory lymphangiogenesis: enhanced production of vascular endothelial growth factor C and D through NF-kappaB activation. *Biochem Biophys Res Commun*. 2008;377:826–831.
8. Randolph GJ, Angeli V, Swartz MA. Dendritic-cell trafficking to lymph nodes through lymphatic vessels. *Nat Rev Immunol*. 2005;5:617–628.
9. Nakao S, Zandi S, Faez S, Kohno RI, Hafezi-Moghadam A. Discontinuous LYVE-1 expression in corneal limbal lymphatics: dual function as microvalves and immunological hot spots. *FASEB J*. 2012;26:808–817.
10. Karpanen T, Alitalo K. Molecular biology and pathology of lymphangiogenesis. *Annu Rev Pathol*. 2008;3:367–397.
11. Nakao S, Hafezi-Moghadam A, Ishibashi T. Lymphatics and lymphangiogenesis in the eye. *J Ophthalmol*. 2012;2012:783163.
12. Junghans BM, Crewther SG, Crewther DP, Pirie B. Lymphatic sinusoids exist in chick but not in rabbit choroid. *Aust N Z J Ophthalmol*. 1997;25(suppl 1):S103–S105.
13. Krebs W, Krebs IP. Ultrastructural evidence for lymphatic capillaries in the primate choroid. *Arch Ophthalmol*. 1988;106:1615–1616.
14. Sugita A, Inokuchi T. Lymphatic sinus-like structures in choroid. *Jpn J Ophthalmol*. 1992;36:436–442.
15. Schroedl F, Brehmer A, Neuhuber WL, Kruse FE, May CA, Cursiefen C. The normal human choroid is endowed with a significant number of lymphatic vessel endothelial hyaluronate receptor 1 (LYVE-1)-positive macrophages. *Invest Ophthalmol Vis Sci*. 2008;49:5222–5229.
16. Xu H, Chen M, Reid DM, Forrester JV. LYVE-1-positive macrophages are present in normal murine eyes. *Invest Ophthalmol Vis Sci*. 2007;48:2162–2171.
17. Nakao S, Maruyama K, Zandi S, et al. Lymphangiogenesis and angiogenesis: concurrence and/or dependence? Studies in inbred mouse strains. *FASEB J*. 2010;24:504–513.
18. Tammela T, Zarkada G, Wallgard E, et al. Blocking VEGFR-3 suppresses angiogenic sprouting and vascular network formation. *Nature*. 2008;454:656–660.
19. Grimaldo S, Garcia M, Zhang H, Chen L. Specific role of lymphatic marker podoplanin in retinal pigment epithelial cells. *Lymphology*. 2010;43:128–134.
20. Cao Y, Linden P, Farnebo J, et al. Vascular endothelial growth factor C induces angiogenesis in vivo. *Proc Natl Acad Sci U S A*. 1998;95:14389–14394.
21. Clarijs R, Schalkwijk L, Ruiter DJ, de Waal RM. Lack of lymphangiogenesis despite coexpression of VEGF-C and its receptor Flt-4 in uveal melanoma. *Invest Ophthalmol Vis Sci*. 2001;42:1422–1428.
22. Chung ES, Chauhan SK, Jin Y, et al. Contribution of macrophages to angiogenesis induced by vascular endothelial growth factor receptor-3-specific ligands. *Am J Pathol*. 2009;175:1984–1992.
23. Gragoudas ES, Adamis AP, Cunningham ET Jr, Feinsod M, Guyer DR. Pegaptanib for neovascular age-related macular degeneration. *N Engl J Med*. 2004;351:2805–2816.
24. Rosenfeld PJ, Brown DM, Heier JS, et al. Ranibizumab for neovascular age-related macular degeneration. *N Engl J Med*. 2006;355:1419–1431.
25. Ip MS, Scott IU, Brown GC, et al. Anti-vascular endothelial growth factor pharmacotherapy for age-related macular degeneration: a report by the American Academy of Ophthalmology. *Ophthalmology*. 2008;115:1837–1846.
26. Brown DM, Heier JS, Ciulla T, et al. Primary endpoint results of a phase II study of vascular endothelial growth factor trap-eye in wet age-related macular degeneration. *Ophthalmology*. 2011;118:1089–1097.
27. Karpanen T, Egeblad M, Karkkainen MJ, et al. Vascular endothelial growth factor C promotes tumor lymphangiogenesis and intralymphatic tumor growth. *Cancer Res*. 2001;61:1786–1790.
28. Nussenblatt RB, Ferris F III. Age-related macular degeneration and the immune response: implications for therapy. *Am J Ophthalmol*. 2007;144:618–626.
29. Killer HE, Laeng HR, Groscurth P. Lymphatic capillaries in the meninges of the human optic nerve. *J Neuroophthalmol*. 1999;19:222–228.
30. Halin C, Tobler NE, Vigl B, Brown LF, Detmar M. VEGF-A produced by chronically inflamed tissue induces lymphangiogenesis in draining lymph nodes. *Blood*. 2007;110:3158–3167.